Chapter 8

Ensemble and Single Quantum Dot Fluorescence Methods in Neurotransmitter Transporter Research

Oleg Kovtun and Sandra J. Rosenthal

Abstract

Subcellular localization and trafficking of neurotransmitter transporter (NTT) proteins is increasingly recognized to play a critical role in transporter-mediated neurotransmitter signaling and its regulation. To fully understand the molecular mechanisms underlying transporter regulation, it is essential to be able to visualize NTTs both at the population and single-molecule levels using advanced imaging techniques. Here, we describe three fluorescence-based methods that have been successfully applied to measure spatiotemporal changes in NTT localization and to establish dynamic imaging of individual NTT molecules using the ligand-conjugated quantum dot (QD) approach. First, we discuss how to label and image membrane NTTs in live cells using QD probes in conjunction with ensemble fluorescence microscopy. Second, we present a more quantitative, flow cytometry-based approach, particularly useful for assessing transporter internalization and recycling. Third, we describe a single-molecule microscopy labeling protocol for determining the mobility of QD-bound transporters at the plasma membrane of live cells.

Key words Quantum dot, Biological labeling, Neurotransmitter transporter, Confocal fluorescence microscopy, Flow cytometry, Biotinylated ligand, Single-molecule imaging

1 Introduction

Traditional biochemical and genetic approaches have contributed the majority of the existing research knowledge on NTT structure, function, and regulation. It is now apparent that NTT function is tightly regulated through multiple posttranslational mechanisms including interactions with a plethora of kinases, receptors, and scaffolding elements [1–5]. Consequent dynamic changes in NTT subcellular localization fundamentally impact the amplitude, duration, and specificity of NTT-mediated neurotransmitter signaling. Therefore, the ability to "see" NTTs with subcellular resolution and to monitor dynamic trafficking pathways involved in NTT regulation becomes a critical tool in advancing our understanding of the molecular mechanisms underlying NTT signaling network.

Heinz Bönisch and Harald H. Sitte (eds.), *Neurotransmitter Transporters: Investigative Methods*, Neuromethods, vol. 118,
DOI 10.1007/978-1-4939-3765-3_8,

Recent advances in fluorescence-based techniques for molecular biology permitted investigation of cellular signal transduction cascades with unprecedented spatiotemporal resolution [6, 7]. Currently, there are several classes of fluorescent probes available to investigators. Among these, the most prevalent fluorophores are organic dyes, genetically encoded fluorescent proteins, and semiconductor nanocrystals, colloquially known as quantum dots (QDs) [8–15]. General properties, advantages, and drawbacks of the aforementioned fluorophores are summarized in Table 1. Our group is primarily focused on exploiting the unique photophysical properties of QDs (excellent brightness, narrow emission spectra, broad excitation spectra, and superior photostability) to study subcellular distribution and dynamic regulation of NTTs [16–24].

There are several methodological approaches to enable specific targeting of membrane proteins in live cells with the aforementioned fluorescent probes (Table 2). Most commonly, (1) a fluorescent protein (e.g., EGFP) is fused to the terminus of the target protein and expressed in the cell of interest, or (2) a fluorophore is attached to an antibody targeting the extracellular domain of the target protein. Unfortunately, limited availability of such extracellular antibodies for NTTs and lack of suitable extracellular epitopes within the NTT structure have significantly hampered fluorescence-based investigation of NTT localization and regulation, particularly in endogenous systems. To this end, we pioneered a ligand-conjugated QD-based approach that utilizes a transporter-specific organic ligand composed of (1) a high-affinity parent drug that enables recognition of specific binding sites within the

Table 1
Comparison of commonly encountered fluorescent probes

Property	Cy5	EGFP	QD655
Size	~0.5 nm; 792 Da	~5 nm; ~27 kDa	15–25 nm; >1000 kDa
Quantum yield	0.3	0.6	0.5
Molar absorption coefficient	2.5×10^5 M^{-1} cm^{-1}	5.6×10^4 M^{-1} cm^{-1}	$>2 \times 10^6$ M^{-1} cm^{-1}
Excitation/emission maxima	649/670 nm	488/509 nm	Steady increase toward UV wavelengths starting from absorption onset; emission max at 655 nm, with FWHM ~30 nm
Photostability	5–10 s	5–10 s	Minutes
Applicability to single-molecule imaging	Moderate; limited by poor photostability	Moderate; limited by poor photostability	Excellent; complicated by blinking

Table 2
Methodological approaches that enable specific targeting of neurotransmitter transporters

Approach	Advantages\disadvantages	References
Genetic fusion (XFP; hemagglutinin fusion peptide)	Pros: perfect specificity, biocompatibility, retention of the XFP-target protein construct Cons: incompatibility with endogenous expression systems, misfolding, failure to localize properly, altered activity compared to the wild-type protein	[25–31]
Antibody	Pros: excellent specificity, biocompatibility, low cytotoxicity, compatibility with endogenous expression systems Cons: lack of efficient external antibodies, large size, prone to chemical degradation	[32]
Organic ligand	Pros: targeting specificity and selectivity, binding stability, compatibility with endogenous expression systems, biological activity Cons: sophisticated organic chemistry and rigorous analytical characterization required for preparation, primary binding site occupied	[16–24, 33–36]
Covalent modification	Pros: excellent selectivity, possibility of an inert functional tag, small size Cons: potentially deleterious effects on protein structure and function, organic chemistry knowledge required	[37, 38]

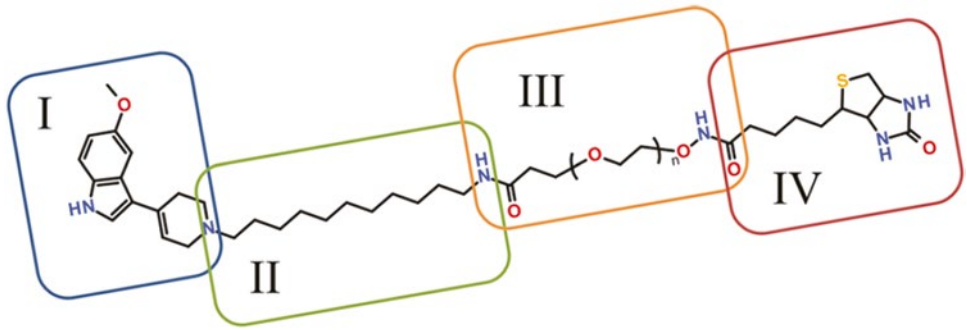

Fig. 1 Structure schematic of tailored organic ligands targeting plasma membrane monoamine transporters. Reprinted with permission from ref. 21. Copyright 2011 American Chemical Society

transporter structure and facilitates pseudo-irreversible binding, (2) a hydrophobic alkyl spacer which permits sufficient flexibility and provides a hydrophobic interface for a successful drug-binding pocket interaction, (3) a PEG polymer that aids in aqueous solubility and abolishes possible nonspecific interactions with the plasma membrane, and (4) a biotin moiety that allows subsequent streptavidin-conjugated QD recognition upon the transporter binding event (Fig. 1) [16–24].

In this chapter, we outline three fluorescence-based techniques that have been successfully applied to measure spatiotemporal changes in NTT localization and to establish dynamic imaging of individual NTT molecules using our ligand-conjugated QD approach. First, we discuss how to label and image membrane NTTs in live cells using QD probes in conjunction with ensemble fluorescence microscopy. Second, we present a more quantitative, flow cytometry-based protocol, particularly useful for assessing transporter internalization and recycling. Third, as dynamic trafficking of NTTs in the plasma membrane appears to be an important post-translational regulatory mechanism, we describe a single-molecule microscopy labeling protocol for determining the mobility of QD-bound transporters in the plasma membrane of live cells.

2 Materials

2.1 HEK293 Cell Culture and Reagents

1. DMEM medium (Gibco, Invitrogen Life Science, Bethesda, MD).
2. Phenol Red-free DMEM medium (Gibco, Invitrogen Life Science, Bethesda, MD).
3. Fetal bovine serum (FBS) (Gemini Bio-Products, West Sacramento, CA).
4. 0.05 % Trypsin/EDTA (Cellgro, Mediatech).
5. L-Glutamine (Gibco, Invitrogen Life Science, Bethesda, MD).
6. T25/T75 flasks; 24-well or 96-well culture plates (BD Biosciences, Falcon).
7. Penicillin (10,000 U/mL) and streptomycin (10 mg/mL) solutions are frozen at –20 °C (Gibco, Invitrogen Life Science); 5 mL is added to 0.5 L of DMEM complete culture medium.
8. Cell line: HEK293 cells transiently or stably expressing NTT of interest.
9. 0.1 mg/mL poly-d-lysine solution in sterile H_2O.
10. Lab-Tek chambered #1.0 borosilicate coverglass (eight-well chamber).
11. Biotinylated ligand (1 mM stock solution in sterile H_2O stored dessicated at –20 °C).
12. Bovine serum albumin (BSA).
13. Streptavidin-conjugated quantum dots (SavQD605), with the emission maximum at 605 nm (Invitrogen Life Science, Bethesda, MD). Optimal filter is HQ 605/20 emission for QD605. QDs can be excited at any wavelengths, but 488 nm is a commonly utilized excitation line to minimize photodamage, QD blinking, and spectral cross-talk.
14. Cell Stripper, nonenzymatic dissociation buffer (Gibco, Invitrogen Life Science, Bethesda, MD).

15. Cell culture incubator, 37 °C, 5 % CO_2.
16. Vacuum pump for cell washes.

2.2 Equipment, Software, and Accessories

1. LSM 510 (Carl Zeiss) or LSM 710 (Carl Zeiss) equipped with a 63× 1.4 NA Apochromat oil-immersion objective lens and a 488-nm excitation line (Ar laser or solid-state diode laser); LSM 510/710 image acquisition/analysis software or ImageJ (NIH image analysis freeware) to process time-lapse and z-stack fluorescence images; microscope-mounted environmental chamber.
2. 3- or 5-laser Becton-Dickinson (BD Biosciences, San Jose, CA) bench-top flow cytometer equipped with a multiwall plate sample cube; 12 × 75 mm polystyrene flow cytometry tubes (BD Biosciences, San Jose, CA); FlowJo flow cytometry data analysis package (TreeStar, Ashland, OR).
3. High-speed, line-scanning Zeiss 5 Live confocal microscope equipped with a 63× 1.4 NA oil-immersion objective lens and a 488-nm 100-mW solid-state diode laser; microscope-mounted environmental chamber; Zeiss LSM Image Examiner software; MatLab or IDL-based programming routines for analysis of real-time QD trajectory data.
4. Imaging medium: phenol red-free DMEM supplemented with 1 % BSA.

3 Methods

For the purpose of this chapter, it is assumed that the NTT of interest is expressed in HEK293 cells; however, the general principles and protocols described below remain valid for any expression system being used.

3.1 Ensemble Microscopy Protocol

1. HEK293 cells are cultured in DMEM supplemented with 10 % FBS, 2 mM l-glutamine, 100 units/mL penicillin, and 100 mg/mL streptomycin and maintained at 37 °C with 5 % CO_2. For ensemble imaging, cells are plated in poly-d-lysine-treated (1 h at 37 °C) eight-well Lab-Tek chambered coverglass at a density of 1×10^5 to 1×10^6 cells/mL and cultured for 24 h prior to imaging.
2. Prior to labeling, wash the cells gently three times with warm phenol red-free culture medium.
3. Incubate cells with a biotinylated ligand (0.1–1 μM) in phenol red-free DMEM for 5–20 min at 37 °C. In the meantime, prepare a SavQD605 labeling by diluting SavQD605 stock solution in warm imaging buffer to reach a desired concentration of (0.5–2 nM) and incubate it in a 37 °C water bath for 10 min.
4. Wash the cells three times with warm phenol red-free DMEM.

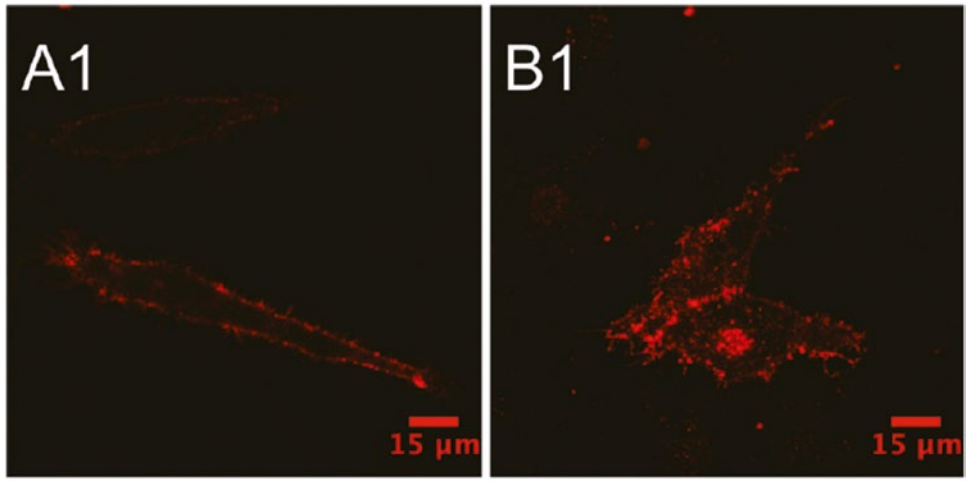

Fig. 2 Labeling of dopamine transporter (DAT) with ligand-conjugated QDots in live cells. (*left*) Streptavidin-conjugated QDots were used to label DATs previously exposed to a biotinylated, PEGylated cocaine analog. (**a1**) QD labeling of membrane DATs in a live HeLa cell. (**b1**) QD-bound DATs underwent acute redistribution from the plasma membrane to intracellular compartments as a result of protein kinase C (PKC) activation. Reprinted with permission from ref. 20. Copyright 2011 American Chemical Society

5. Incubate the cells with SavQD605 solution for 5 min at 37 °C and wash at least three times with warm imaging buffer.
6. Immediately post-labeling, place the chambered coverglass on the microscope with the mounted environmental chamber.
7. Acquire fluorescent images at 37 °C. Example data are shown in Fig. 2.

3.2 Flow Cytometry Protocol

1. Cells are plated in a poly-d-lysine-treated (1 h at 37 °C) 24-well/96-well culture plate at a density of $1–5 \times 10^5$ cells/mL 48 h prior to the flow cytometry assay.
2. Prior to QD conjugate labeling, wash the cells three times with warm DMEM and incubate with a drug for 10–30 min in complete culture medium at 37 °C and 5 % CO_2. Parallel control wells are incubated with either drug-free complete culture medium (positive control) or in the presence of a high-affinity transporter inhibitor (negative control).
3. Wash the cells three times with warm phenol red-free DMEM and incubate with biotinylated ligand (0.1–1 µM)/drug mixture for 10 min at 37 °C in warm phenol red-free DMEM.
4. Wash the cells three times with ice-cold imaging buffer and incubate with previously prepared SavQD605 labeling solution in ice-cold imaging buffer.
5. Wash the cells gently three times with the ice-cold imaging buffer and add Cell Stripper solution. Incubate for 5–10 min at 37 °C.

6. Analyze cell QD fluorescence using a flow cytometer.
7. Data are typically collected from >10,000 cells per sample, with median fluorescence intensity as one of the recorded fluorescent signal parameters.
8. By utilizing median fluorescence intensity (MFI) parameter obtained from control cell populations, it is possible to compute the percentage of DAT molecules unavailable for binding (PI, percent inhibition) according to the equation below:

$$\mathrm{PI} = \frac{\mathrm{MFI}_{\mathrm{pos}} - \mathrm{MFI}_{\mathrm{treated}}}{\mathrm{MFI}_{\mathrm{pos}} - \mathrm{MFI}_{\mathrm{neg}}} \times 100\,\%$$

where $\mathrm{MFI}_{\mathrm{pos}}$ is MFI of a positive control (QD-ligand-labeled cells), $\mathrm{MFI}_{\mathrm{neg}}$ is MFI of a negative control (QD only-labeled cells), and $\mathrm{MFI}_{\mathrm{treated}}$ is MFI of a cell population incubated with a certain DAT modulator dose and subsequently labeled with ligand-conjugated QDs [23]. Example data are shown in Fig. 3.

3.3 Single-Molecule Microscopy Protocol

1. Cells are plated in poly-d-lysine-treated (1 h at 37 °C) eight-well Lab-Tek chambered coverglass at a density of $1–5 \times 10^4$ cells/mL and cultured for 24 h prior to imaging.
2. Prior to labeling, wash the cells gently three times with warm phenol red-free culture medium.
3. Incubate cells with a biotinylated ligand (1–100 nM) in phenol red-free DMEM for 5–20 min at 37 °C. In the meantime, prepare a SavQD605 labeling by diluting SavQD605 stock solution in warm imaging buffer to reach a desired concentration of (0.01–0.5 nM) and incubate it in a 37 °C water bath for 10 min.
4. Wash the cells three times with warm phenol red-free DMEM.
5. Incubate the cells with SavQD605 solution for 5 min at 37 °C and wash thoroughly at least three times with warm imaging buffer to remove unbound QDs.
6. Immediately post-labeling, place the chambered coverglass on the microscope with the mounted environmental chamber.
7. Acquire time-lapse fluorescent images at 37 °C immediately after the final wash step. Typically, the final wash step is carried in the immediate vicinity of the imaging system.
8. Live imaging should not exceed 30 min at 37 °C for cell survival and is optimally carried out within the initial 10–15 min to limit turnover of QD-bound membrane NTT molecules.
9. Real-time, time-lapse image recording is obtained with an integration time of 25–100 ms for at least 500 consecutive frames. Example series are shown in Fig. 4.

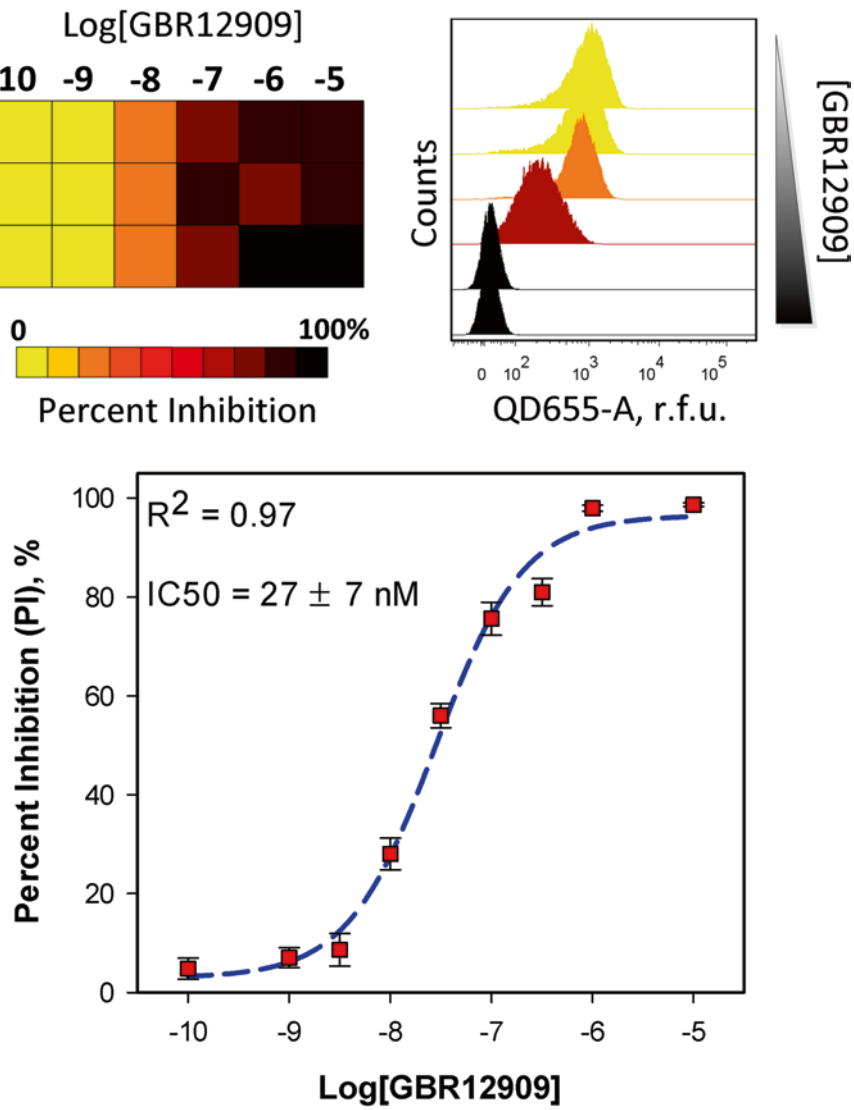

Fig. 3 Flow cytometry-based screening of the inhibitory activity of GBR12909, a high-affinity DAT antagonist, using antagonist-conjugated Qdots. DAT-expressing HEK cells were treated with five- or tenfold dilutions of GBR12909. Percent inhibition at increasing doses of GBR12909 is represented as a heat map (*top left*) and representative histogram plots of the effects of increasing GBR12909 doses (*top right*) on QD conjugate binding are shown. The heat map and IC50 curve (*bottom*) were generated using median QD fluorescence intensity values. Reprinted with permission from ref. 23. Copyright 2012 Royal Chemical Society

10. Real-time trajectory data is subsequently obtained from the recorded time-lapse image series and analyzed using custom programs written in Matlab or IDL programming software. Tracking analysis sequence is illustrated in Fig. 5.

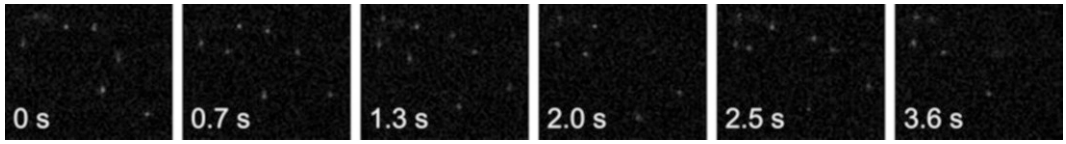

Fig. 4 Time-lapse image series depicting movement of cell surface QD-bound transporters

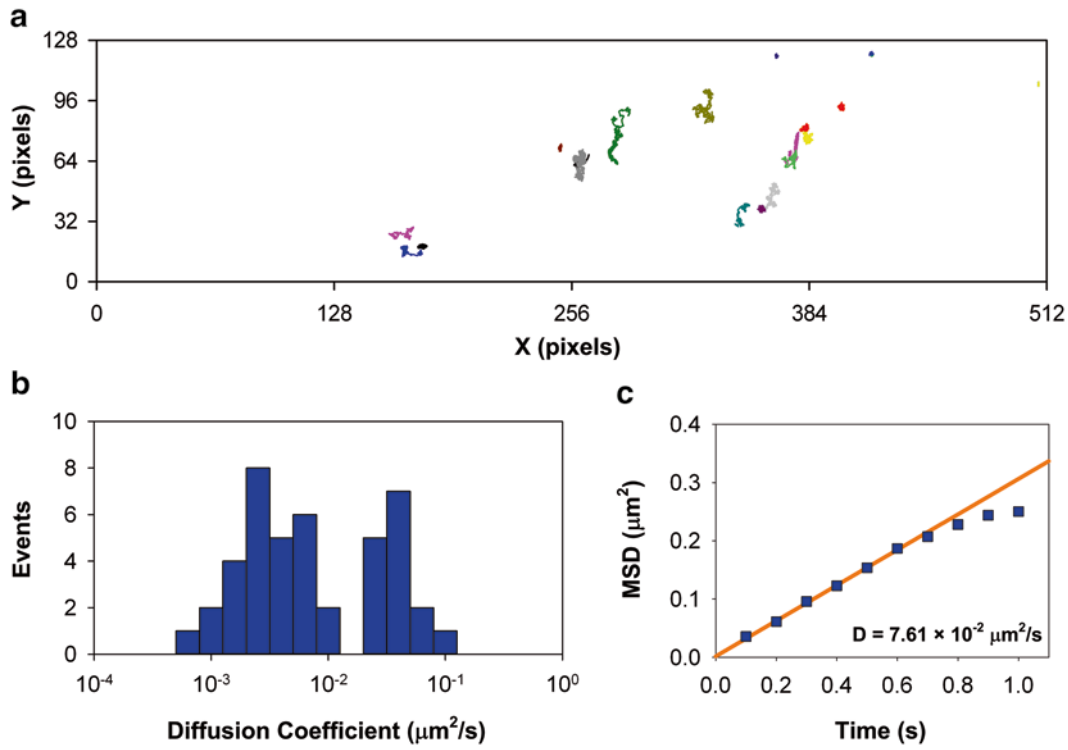

Fig. 5 Schematic illustrating trajectory data analysis in a typical single-QD tracking experiment. (**a**) Example of QD-DAT trajectories on the surface of transfected HEK293 cells. Scale: 1 pixel = 200 nm. (**b**) A histogram showing diffusion coefficients determined for the trajectories in **a**. (**c**) Averaged mean square displacement (MSD)-time plot of QD trajectories. Ensemble diffusion coefficient is estimated via the linear fit of 2–5 MSD-time plot data points

4 Notes

1. Optimal plating density and cell health are critical to keep weakly adherent cells, such as HEK293, from detaching off the Lab-Tek chambered coverglass throughout the protocol. Treatment of the chambered coverglass with poly-d-lysine solution is a necessary step to ensure the cells remain adhered to the glass bottom through the extensive series of incubation and wash steps. Also, it is of utmost importance that one carefully examines cell morphology and overall cell health prior to acquiring fluorescence data.

2. One of the most important variables for a successful experiment is adequate quality and quantity of washings after drug, biotinylated ligand, and QD incubation. One must wash extensively after each separate step to remove excess, unbound probes, as they have the potential to interfere with subsequent recognition events and ultimately affect the specificity of QD labeling. Additionally, it is imperative that one always prepares fresh working solutions the day of the experiment.
3. The most critical determinant of experimental success is the specificity of biotinylated ligand binding. One must find optimal ligand concentration and incubation time to maximize specific binding. In our experience, 0.1–1 μM and 5–20 min ranges for ligand dose and incubation time respectively are typically a good starting point. In all cases, one must run parallel control samples to ensure labeling specificity. The control samples usually are to (1) apply the same labeling conditions to parental cells not expressing the transporter of interest, (2) include a high-affinity inhibitor to block the specific binding site during the labeling protocol, and (3) label transporter-expressing cells with only the QD probes to assess the degree of nonspecific QD binding and the effectiveness of wash steps.
4. Another important aspect of assuring labeling specificity is the addition of a common blocking agent, such as BSA, to the QD solution and the imaging buffer. QD nonspecific binding varies significantly among cell types, and one must take great care to optimize the blocking conditions (Fig. 6). Common blocking reagents are BSA, FBS, horse serum, gelatin, and nonfat dry milk.
5. As QD-bound NTTs are subject to dynamic protein turnover, fluorescence data acquisition must be conducted immediately after the final wash step, especially in the case of single-

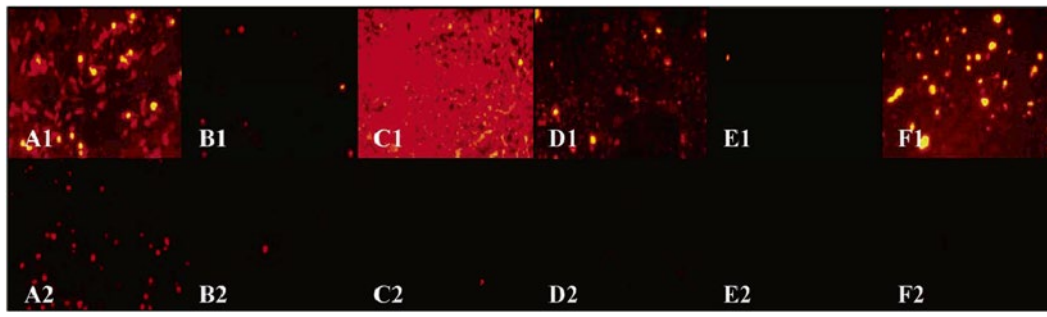

Fig. 6 Comparison of nonspecific cell surface binding of 50 nM AMP™ Dots (**a1**–**f1**) and PEGylated AMP™ Dots (**a2**–**f2**). Nonspecific binding was found to be dependent upon the cell type, and conjugation of methoxy-terminated PEG2000 to the surface of AMP™ Dots resulted in significant reduction of nonspecific cellular binding. Figure reproduced with permission from ref. 40. Copyright 2005 American Chemical Society

molecule experiments. This helps prevent transporter endocytosis and allows adequate visualization of membrane-restricted signaling events.

6. An important consideration is controlling the valency of the binding. This is a particularly critical parameter in single-molecule experiments, as multivalent QD labeling leads to protein cross-linking that may inadvertently trigger downstream signal transduction cascades. To this end, there are two common solutions. One involves preincubation of SavQDs with the biotinylated ligand at ~1:1 ratio in a borate buffer (pH ~8.5) for 0.5–24 h at room temperature with constant stirring; the other involves a two-step labeling protocol as described above and the use of ~equimolar doses of biotinylated ligand and SavQDs. In the case of endogenous expression systems, this requirement can be relaxed, as the low surface density of transporters is the primary determinant of monovalent labeling.
7. QD density must be adjusted accordingly to ensure maximum signal-to-noise ratio in ensemble imaging and permit observation of 10–20 individual QDs on the cell surface in a single-molecule experiment. This is achieved via titrating the QD concentration while keeping the concentration of biotinylated ligand constant.
8. Table 3 provides a set of troubleshooting instructions for a typical single-molecule experiment [39].

Table 3

Troubleshooting a single-QD imaging experiment

Problem	Cause	Solution
Low or excessive QD label density	Inappropriate biotinylated ligand concentration	Optimize ligand concentrations for labeling
	Poor or excessive transporter expression	Check whether the transporter is delivered to the surface. Optimize protein expression level
	QD aggregation	Prepare fresh QD dilution and store for no longer than a few hours
	Poor ligand affinity	Check ligand affinity via transport uptake assay
Nonspecific labeling	Excessive ligand or QD concentration	Reduce and optimize ligand and QD concentrations
Excessive QD blinking	Excessive excitation duration or intensity	Minimize excitation intensity, use longer wavelengths, and reduce the excitation duration

Acknowledgements

The authors wish to thank Prof. Randy D. Blakely, Dr. Jerry C. Chang, and Dr. Ian D. Tomlinson for all the helpful discussions and suggestions. This work was supported by grants from National Institutes of Health EB003728 to S.J.R. O.K. would also like to acknowledge Vanderbilt Institute for Nanoscale Science and Engineering (VINSE) fellowship.

References

1. Torres GE, Gainetdinov RR, Caron MG (2003) Plasma membrane monoamine transporters: structure, regulation and function. Nat Rev Neurosci 4(1):13–25
2. González MI, Robinson MB (2004) Neurotransmitter transporters: why dance with so many partners? Curr Opin Pharmacol 4(1):30–35
3. Sager JJ, Torres GE (2011) Proteins interacting with monoamine transporters: current state and future challenges. Biochemistry 50(34): 7295–7310
4. Fei H, Grygoruk A, Brooks ES, Chen A, Krantz DE (2008) Trafficking of vesicular neurotransmitter transporters. Traffic 9(9):1425–1436
5. Ramamoorthy S, Shippenberg TS, Jayanthi LD (2011) Regulation of monoamine transporters: role of transporter phosphorylation. Pharmacol Ther 129(2):220–238
6. Haraguchi T (2002) Live cell imaging: approaches for studying protein dynamics in living cells. Cell Struct Funct 27(5): 333–334
7. Sako Y, Yanagida T (2003) Single-molecule visualization in cell biology. Nat Rev Mol Cell Biol (Suppl): SS1–SS5
8. Resch-Genger U, Grabolle M, Cavaliere-Jaricot S, Nitschke R, Nann T (2008) Quantum dots versus organic dyes as fluorescent labels. Nat Methods 5(9):763–775
9. Lippincott-Schwartz J, Patterson GH (2003) Development and use of fluorescent protein markers in living cells. Science 300(5616): 87–91
10. Zhang J, Campbell RE, Ting AY, Tsien RY (2002) Creating new fluorescent probes for cell biology. Nat Rev Mol Cell Biol 3(12):906–918
11. Alivisatos AP, Gu W, Larabell C (2005) Quantum dots as cellular probes. Annu Rev Biomed Eng 7:55–76
12. Bruchez M Jr, Moronne M, Gin P, Weiss S, Alivisatos AP (1998) Semiconductor nanocrystals as fluorescent biological labels. Science 281(5385):2013–2016
13. Chan WC, Nie S (1998) Quantum dot bioconjugates for ultrasensitive nonisotopic detection. Science 281(5385):2016–2018
14. Rosenthal SJ, Chang JC, Kovtun O, McBride JR, Tomlinson ID (2011) Biocompatible quantum dots for biological applications. Chem Biol 18(1):10–24
15. Chang JC, Kovtun O, Blakely RD, Rosenthal SJ (2012) Labeling of neuronal receptors and transporters with quantum dots. Wiley Interdiscip Rev Nanomed Nanobiotechnol 4(6):605–619
16. Rosenthal SJ, Tomlinson I, Adkins EM, Schroeter S, Adams S, Swafford L, McBride J, Wang Y, DeFelice LJ, Blakely RD (2002) Targeting cell surface receptors with ligand-conjugated nanocrystals. J Am Chem Soc 124(17):4586–4594
17. Tomlinson ID, Mason JN, Blakely RD, Rosenthal SJ (2005) Inhibitors of the serotonin transporter protein (SERT): the design and synthesis of biotinylated derivatives of 3-(1,2,3,6-tetrahydro-pyridin-4-yl)-1H-indoles. High-affinity serotonergic ligands for conjugation with quantum dots. Bioorg Med Chem Lett 15(23):5307–5310
18. Tomlinson ID, Mason JN, Blakely RD, Rosenthal SJ (2006) High affinity inhibitors of the dopamine transporter (DAT): novel biotinylated ligands for conjugation to quantum dots. Bioorg Med Chem Lett 16(17):4664–4667
19. Tomlinson ID, Chang J, Iwamoto H, Felice LJD, Blakely RD, Rosenthal SJ (2008) Targeting the human serotonin transporter (hSERT) with quantum dots. SPIE 6866:68660X
20. Kovtun O, Tomlinson ID, Sakrikar DS, Chang JC, Blakely RD, Rosenthal SJ (2011) Visualization of the cocaine-sensitive dopamine transporter with ligand-conjugated quantum dots. ACS Chem Neurosci 2:370–378
21. Chang JC, Tomlinson ID, Warnement MR, Iwamoto H, DeFelice LJ, Blakely RD, Rosenthal SJ (2011) A fluorescence displacement assay for antidepressant drug discovery based on ligand-conjugated quantum dots. J Am Chem Soc 133(44):17528–17531

22. Tomlinson ID, Iwamoto H, Blakely RD, Rosenthal SJ (2011) Biotin tethered homotryptamine derivatives: high affinity probes of the human serotonin transporter (hSERT). Bioorg Med Chem Lett 21(6): 1678–1682
23. Kovtun O, Ross EJ, Tomlinson ID, Rosenthal SJ (2012) A flow cytometry-based dopamine transporter binding assay using antagonist-conjugated quantum dots. Chem Commun 48(44):5428–5430
24. Chang JC, Tomlinson ID, Warnement MR, Ustione A, Carneiro AMD, Piston DW, Blakely RD, Rosenthal SJ (2012) Single molecule analysis of serotonin transporter regulation using antagonist-conjugated quantum dots reveals restricted, p38 MAPK-dependent mobilization underlying uptake activation. J Neurosci 32(26):8919–8929
25. Fjorback AW, Pla P, Müller HK, Wiborg O, Saudou F, Nyengaard JR (2009) Serotonin transporter oligomerization documented in RN46A cells and neurons by sensitized acceptor emission FRET and fluorescence lifetime imaging microscopy. Biochem Biophys Res Commun 380(4):724–728
26. Schmid JA, Scholze P, Kudlacek O, Freissmuth M, Singer EA, Sitte HH (2001) Oligomerization of the human serotonin transporter and of the rat GABA transporter 1 visualized by fluorescence resonance energy transfer microscopy in living cells. J Biol Chem 276(6):3805–3810
27. Furman CA, Chen R, Guptaroy B, Zhang M, Holz RW, Gnegy M (2009) Dopamine and amphetamine rapidly increase dopamine transporter trafficking to the surface: live-cell imaging using total internal reflection fluorescence microscopy. J Neurosci 29(10):3328–3336
28. Egaña LA, Cuevas RA, Baust TB, Parra LA, Leak RK, Hochendoner S, Peña K, Quiroz M, Hong WC, Dorostkar MM, Janz R, Sitte HH, Torres GE (2009) Physical and functional interaction between the dopamine transporter and the synaptic vesicle protein synaptogyrin-3. J Neurosci 29(14):4592–4604
29. Gränäs C, Ferrer J, Loland CJ, Javitch JA, Gether U (2003) N-terminal truncation of the dopamine transporter abolishes phorbol ester- and substance P receptor-stimulated phosphorylation without impairing transporter internalization. J Biol Chem 278(7):4990–5000
30. Sorkina T, Richards TL, Rao A, Zahniser NR, Sorkin A (2009) Negative regulation of dopamine transporter endocytosis by membrane-proximal N-terminal residues. J Neurosci 29(5):1361–1374
31. Rao A, Richards TL, Simmons D, Zahniser NR, Sorkin A (2012) Epitope-tagged dopamine transporter knock-in mice reveal rapid endocytic trafficking and filopodia targeting of the transporter in dopaminergic axons. FASEB J 26(5):1921–1933
32. Rao A, Simmons D, Sorkin A (2011) Differential subcellular distribution of endosomal compartments and the dopamine transporter in dopaminergic neurons. Mol Cell Neurosci 46(1):148–158
33. Hadrich D, Berthold F, Steckhan E, Bönisch H (1999) Synthesis and characterization of fluorescent ligands for the norepinephrine transporter: potential neuroblastoma imaging agents. J Med Chem 42(16):3101–3108
34. Cha JH, Zou M-F, Adkins EM, Rasmussen SGF, Loland CJ, Schoenenberger B, Gether U, Newman AH (2005) Rhodamine-labeled 2β-carbomethoxy-3β-(3,4-dichlorophenyl)tropane analogues as high-affinity fluorescent probes for the dopamine transporter. J Med Chem 48(24):7513–7516
35. Eriksen J, Rasmussen SGF, Rasmussen TN, Vaegter CB, Cha JH, Zou M-F, Newman AH, Gether U (2009) Visualization of dopamine transporter trafficking in live neurons by use of fluorescent cocaine analogs. J Neurosci 29(21):6794–6808
36. Zhang P, Jørgensen TN, Loland CJ, Newman AH (2013) A rhodamine-labeled citalopram analogue as a high-affinity fluorescent probe for the serotonin transporter. Bioorg Med Chem Lett 23(1):323–326
37. Li M, Lester HA (2002) Early fluorescence signals detect transitions at mammalian serotonin transporters. Biophys J 83(1):206–218
38. Zhao Y, Terry D, Shi L, Weinstein H, Blanchard SC, Javitch JA (2010) Single-molecule dynamics of gating in a neurotransmitter transporter homologue. Nature 465(7295):188–193
39. Bannai H, Levi S, Schweizer C, Dahan M, Triller A (2007) Imaging the lateral diffusion of membrane molecules with quantum dots. Nat Protoc 1(6):2628–2634
40. Bentzen EL, Tomlinson ID, Mason J, Gresch P, Warnement MR, Wright D, Sanders-Bush E, Blakely R, Rosenthal SJ (2005) Surface modification to reduce nonspecific binding of quantum dots in live cell assays. Bioconjug Chem 16(6):1488–1494